A Study on the Flow Characteristics in a Torque Converter
토크 컨버터 유동특성에 대한 연구

S. C. Yoo and S. K. Jang
유성출·장성국

(received 17 September 2007, revised 12 January 2008, accepted 12 February 2008)

주요용어 : 토크 컨버터(Torque Converter), 레이저 도플러 속도 측정장치(LDV), 임펠러(Impeller), 터빈(Turbine), 속도비(Speed Ratio), 관측창(Window)

요 약 : 양산되는 승용차용 토크 컨버터 내부의 유동을 LDV 측정 기술을 이용하여 정량화했다. 속도비 0.4와 0.8 경우에 대한 속도 측정을 통해 임펠러 유로 중간과 출구 영역의 질량 유동율 특성을 분석했다. 측정단면의 속도 분포는 유로의 위치와 속도비에 따라 많은 차이를 보이며, 특히 속도비 0.8 조건에서 임펠러 유로 중간영역 흡입면 부근의 유동은 유동박리에 의한 재순환 현상을 나타내며, 이와는 대조적으로 출구 영역에서는 흡입면을 따라 역류 현상이 발생한다. 임펠러 유로 내부의 유동은 각 영역에서 속도비에 따라 개별적 유동 특성을 보인다. 질량 유동율은 모든 속도비와 측정단면에서 주기적인 변화를 보이며, 또한 터빈의 순간적인 위치가 임펠러 유로 측정단면의 질량 유동율에 매우 큰 영향을 미치는 것이 밝혀졌다. 따라서 토크 컨버터 임펠러의 유로 방향 유동 특성 변화는 컨버터 설계에 중요하게 고려되어야 할 것으로 보인다.

Nomenclature

N_i : input speed
T_i : input torque

1. Introduction

The torque converter has three important functions. The first is that it must transfer power smoothly and efficiently from the engine to the transmission. Second, the torque converter must have the ability to multiply engine torque for improved vehicle launching at low speeds. Third, it must be able to effectively dampen engine torsional vibrations and shock loads. The automotive torque converter is made up of several components. The impeller, also known as a pump, is attached directly to the cover. The cover, in turn, is connected to a flexiplate, which is attached to the engine, and rotates at engine speed. When the converter is rotating fluid exits the impeller and impacts the turbine causing it to rotate. The turbine is driven by the impeller and rotates on its own axis driving the transmission input shaft. The stator is positioned between the impeller and turbine and redirects the fluid flow from the turbine to the impeller.

Torque converter flow fields are extremely complex, in that they contain three-dimensional flows, are viscous, and unsteady. To add to the complexity, the difference in rotor speeds between the impeller and turbine compound the flow effects. There have been numerous studies on the operation of torque converters from CFD, pitot tube analysis to LDV measurements.[1-8] These were designed to understand fluid flow characteristics and improve torque converter performance. The shortcoming was few of the studies were performed in an actual automotive torque converter in realistic operating conditions.

유성출(책임저자) : 한라대학교 기계자동차공학부
E-mail : scyoo@halla.ac.kr Tel. 033-760-1215
장성국 : 한라대학교 기계자동차공학부

The objectives of this study center on design technology improvements. Specific objectives include improving performance of the torque converter and reducing fuel consumption in urban use. To be able to achieve these objectives a thorough understanding of the fluid flow's dynamic phenomena is essential. The use of Laser Doppler Velocimetry (LDV) measurements make it possible to examine the internal flow characteristics of the torque converter.[9] The mass flow rate data series were processed using the measured velocity data. All of the turbine angles were ensemble averaged at each measured impeller position. This result would show the primary characteristics of the toroidal flow and can be used for flow comparison of experimental results with those of the CFD results. The overall efficiency of the torque converter may be improved by optimizing flow fields measured using internal flow diagnostics.

LDV measurements were conducted at a total of two planes. The first plane (Plane 1) was measured at mid-chord between the entrance and exit in the impeller passage. The purpose of making measurements in this plane was to study the uniformity of the flow as it continues toward the impeller exit. The second plane (Plane 2) was measured at the exit of the impeller passage. The purpose of making measurements this plane was to study the fluid flow as it continues from the impeller exit out into the gap region. The measurements were conducted under two operating conditions, which were speed ratios of 0.4 and 0.8. The 0.4 speed ratio has an impeller speed of 1600 rpm and a turbine speed of 633 rpm, while the impeller speed is 2000 rpm and the turbine speed is 1600 rpm for the 0.8 speed ratio.

2. Experimental facility and procedure

2.1 Test rig and control system

Automotive production torque converter has been modified to allow for access to the inside of the converter as well as the addition of Plexiglas window. The window provides optical access to the flows within the impeller passage, exit and the gap between the impeller and turbine blades. The inside surface of the window follows the curvature of the inside surface of the converter housing, so that fluid flow inside the converter should not be disturbed. Due to the complex geometry of the inside surface of the window, the LDV measurement required that the refractive index of the material used for the window must be closed to that of the transmission oil.

The test rig assembly consists of a torque converter fixture, a bedplate, a 40 kW DC drive motor and a 40 kW Universal Dynamometer. A schematic of this test rig assembly is shown in Fig. 1. The converter fixture supports the modified torque converter and allows optical access into the torque converter for flow studies. The bedplate is used to support the fixture assembly with a fixture bracket. The drive motor was used to simulate the engine output, while the Universal Dynamometer simulated the load conditions placed on the torque converter. The drive motor can produce a maximum of 2500 rpm, and is geared at 2:1 ratio to that of the torque converter impeller, resulting in a converter speed of 5000 rpm. The Universal Dynamometer is at a 1:1 ratio and drives the converter turbine at 5000 rpm.

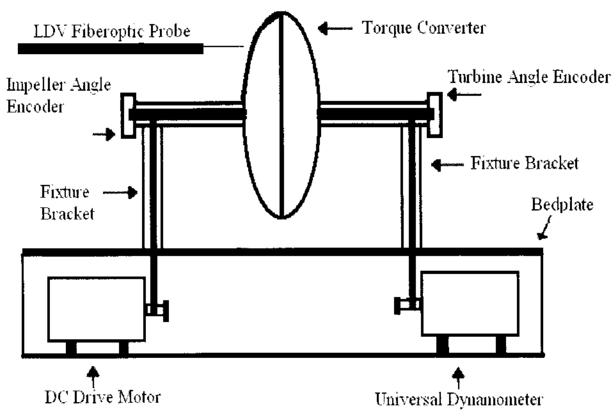

Fig. 1 Schematic of test rig assembly

The output side bearing assembly features the transmission oil flow in and out of the torque converter, as well as access to the bearings for oil lubrication. The design of the bearing assemblies includes strain gauges attached to the impeller, the turbine and the stator. This allows for input and output torques to be recorded in real time. At the either end of the bearing assemblies, a set of angle encoders were installed to determine the relative angular location during rotation. The angle resolution of the encoders is 0.09°CA.

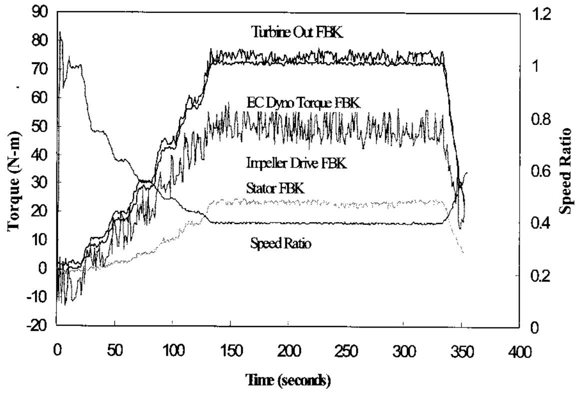

(a)

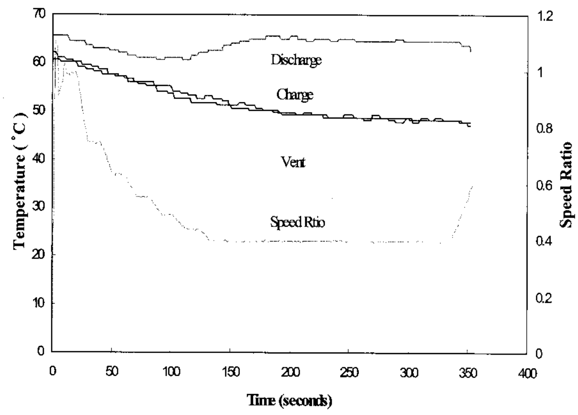

(b)

Fig. 2 Torque measurements (a) and recorded temperature (b)

It has been noticed that operating the torque converter steadily is a key to the success of this experimental study. A computer control system was employed to keep the impeller and turbine speeds constant within less than ±1 rpm in operating conditions. The controller monitors transmission oil flow rates, pressures, and temperatures. The conditions held at steady state for the measurements taken can be seen in Table 1. It also measures input and feedback torque from the impeller, turbine, and stator shafts. All those monitored, measured and calculated data were stored in the computer. Fig. 2 shows a set of recorded data stored in computer. The graphs show the controller keep the torque and temperature constant during the measurements.

Table 1 Conditions used for the flow measurements

0.4 Speed Ratio			0.8 Speed Ratio		
Oil Temp. (℃)		Pressure (kPa)	Oil Temp. (℃)		Pressure (kPa)
Vent	40	521.4	Vent	30	525.1
Charge	40	412.5	Charge	30	449.3
Discharge	65	233.5	Discharge	50	253.7

2.2 LDV system

Velocity measurements from within the torque converters were made using LDV. Elements making up the LDV system include an Argon-ion laser, colorburst and 4-beam fiberoptic probe using a lens with a 350 mm focal length. A frequency shifter, digital burst correlator (IFA-750), traverse table allowing for three degrees of translation and one degree rotation and a PC for data collection and storage are also required for this experiment.

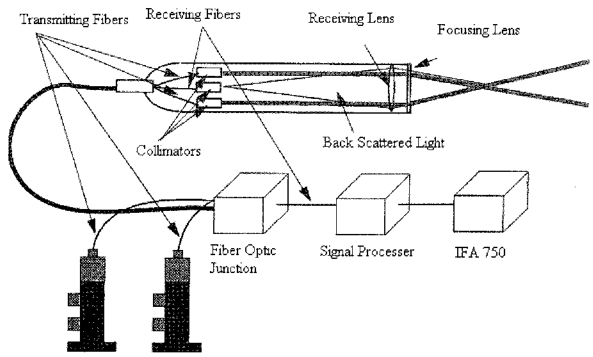

Fig. 3 Back scatter schematic

The scattered light is collected by a photomultiplier. The function of the photomultiplier is to convert bursts of light scattered in the fringe pattern into an analog signal for interpretation by the data acquisition equipment (IFA-750). The data acquisition equipment then combines the frequency of the analog signals with a set of encoder values relating to the position of the impeller and turbine. Each encoder generates one square pulses per evolution. A total of 4096 pulses per revolution were used. This related data set is stored in a PC connected to the data acquisition hardware. A schematic of these events can be seen in Fig. 3. The schematic shows a back-scattering system, where the bursts of light scattered from the measurement volume are collected at a physical location in front of the focal point. In back-scattering mode, the intensity of scattered light is one thousand times weaker than scattered light intensity using the forward-scattering method. Back-scattering data collection was used in this experiment due to optical access constraints.

2.3 Experimental procedure

Production torque converter was modified to install window for optical access for the internal flow study. To verify that the modified converter operates in a same performance behavior, a series of constant input performance tests were run at 67.8 N·m (50 ft·lb) of constant input torque. The test was conducted for the turbine speed range of 400 to 2000 rpm. The pressures, temperatures, flow rates of oil circulation, and torque on each shaft were recorded, so that the K-factor and efficiency of modified converter can be compared with values from the unmodified converter. The K-factor is used to determine the "capacity" of a particular torque converter design. The K-factor is represented by the relation in equation 1. In this equation, N_i and T_i are input speed and input torque respectively. This relationship is used over the full range of torque converter operation.

$$K = \frac{N_i}{\sqrt{T_i}} \tag{1}$$

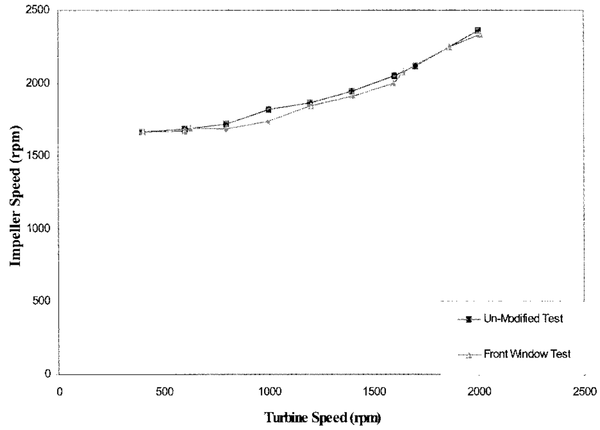

(a) Impeller and turbine speed comparison

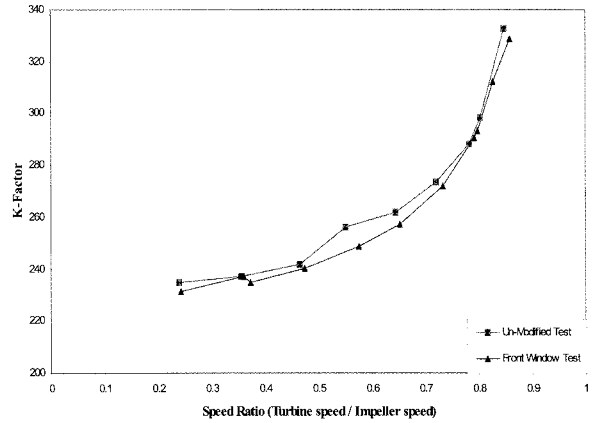

(b) K-factor comparison

Fig. 4 Comparisons of the constant input performance test results

The results of the test and the comparison of the K-factors are shown in Fig. 4. The maximum deviation of the turbine speed was less than 6% and the K-factors were well matched with that from the unmodified converter less than 5% error.

Quantitative internal flow measurements were conducted using multi-components LDV system. It is difficult task to measure velocity at a point in a torque converter. The flow inside the converter is highly turbulence and complicated structured three-dimensional. In addition, the converter has complex structure. In a converter housing, impeller, turbine and stator exist together and all of them rotate in different speed independently. Two angle encoders were installed for impeller and turbine shafts to quantify the flows with the relative positions of impeller and turbine.

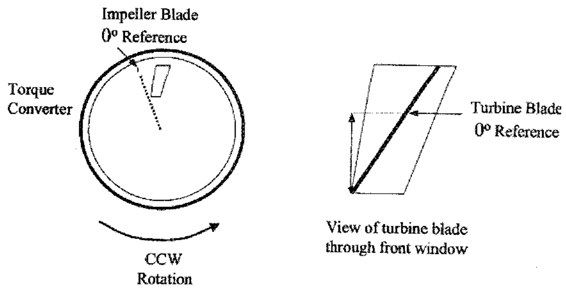

Fig. 5 View of impeller and turbine positions for encoder references

The encoder zero degree reference points are set by use of the LDV laser beams, angle encoders and also an oscilloscope (Fig. 5). For the impeller the welding tab on the shell of the converter of the following impeller blade is used, whereas, for the turbine the surface of the turbine blade itself is used. Once the beams are oriented the shaft encoder trigger signal is viewed on the oscilloscope and the encoder is then set.

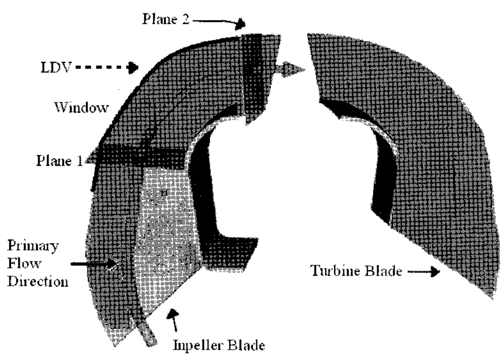

Fig. 6 View of impeller and turbine blades inside the torque converter with measured planes

Two planes were measured at different locations in the impeller passage. The planes were chosen to be perpendicular to the centerline of the passage. The measured planes in the impeller passage are located at 91.5 mm in radius (Plane 1) and 1 mm (Plane 2) inside from the exit of impeller passage. The measured planes with the view of impeller and turbine blades are shown in Fig. 6.

3. Results and discussion

The mass flow rates at two planes were calculated with measured velocities. It was difficult to compare the mass flow rate results of Plane 1 and 2 due to the limited amount of area each measured. The data measured showed the effect of instantaneous turbine blade positions on the primary flow direction inside impeller passage. This was an attempt to map flow characteristics in torque converter operating conditions.

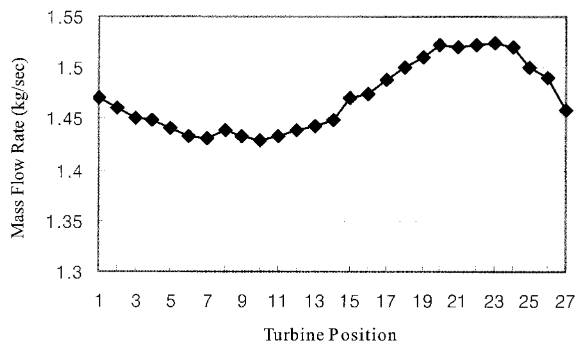

Fig. 7 Mass flow rate data from Plane 1 for the 0.4 speed ratio

The mass flow rate results from Plane 1 for the 0.4 speed ratio can be seen in Fig. 7. This plot represents the extrapolated values of the mass flow rate over the measurement area of the passage orthogonal to the streamwise flow. A single period sinusoid can be seen over the 27 turbine positions for plane. The amplitude of sinusoid amounts to a 7% variation of the flow rate from the average flow for the 27 turbine positions. The lowest flow rate occurs when 33% of the turbine passage width has rotated across the exit of the impeller passage. The highest flow rate occurs at 66% of this same distance. The frequency of the sinusoid corresponds to the frequency of the passing of the turbine blades in front of the impeller exit at every 0.062 second intervals.

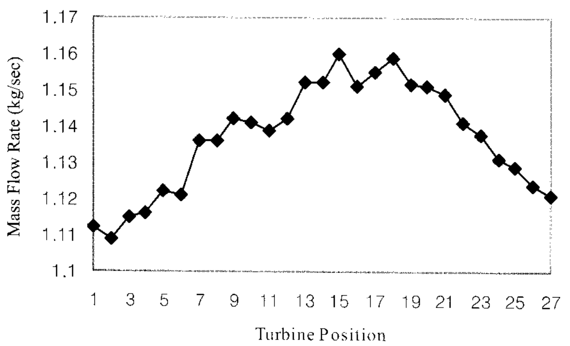

Fig. 8 Mass flow rate data from Plane 1 for the 0.8 speed ratio

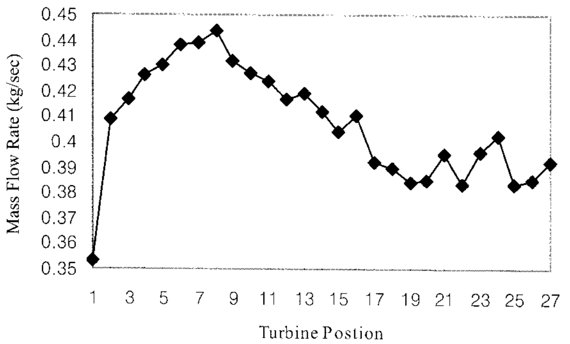

Fig. 9 Mass flow rate data from Plane 2 for the 0.4 speed ratio

Plane 1 for the 0.8 speed ratio data also exhibits similar sinusoid in the mass flow rate calculations, seen in Fig. 8. The variation in mass flow rate due to the amplitude compared to the average mass flow rate of the sinusoid is 5% for 0.8 speed ratio. There is less fluctuation in the flow rate for the 0.8 speed ratio data than the 0.4. This could be due to the reduction in flow rate or the reduction of rigorous mixing. These effects would be caused by the low relative speed of the turbine to the impeller blade. The frequency of the sinusoid coincides with the rate of turbine blades crossing the exit of the impeller passage. The maximum flow rate occurs with the turbine rotated 50% of its passage width across the impeller passage. Minimum flow rate occurs when the turbine blades lie on either side of the impeller passage.

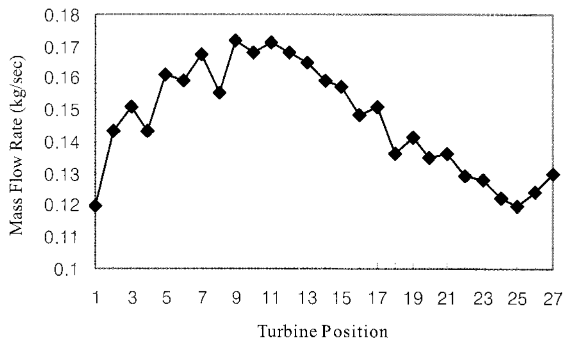

Fig. 10 Mass flow rate data from Plane 2 for the 0.8 speed ratio

The mass flow rate data for Plane 2 at the 0.4 and 0.8 speed ratio conditions displays a similar sinusoidal trend. Plane 2 for the 0.4 speed ratio, seen in Fig. 9, has a maximum value of 0.44 kg/sec and a minimum of 0.35 kg/sec. The minimum value appears as a discontinuity in the data set. The minimum value observed on the sinusoidal trend in this data set is 0.38 kg/sec. The percent variation about the average mass flow rate of 0.405 kg/sec is 15%. The maximum value occurs when 33% of the turbine passage width has crossed in front of the impeller passage exit. The minimum occurs at 66% of this same distance.

The mass flow rate data from Plane 2 for the 0.8 speed ratio, seen in Fig. 10, has a minimum value of 0.12 kg/sec and a maximum of 0.17 kg/sec. The average mass flow rate for the 27 turbine positions resolved is 0.145 kg/sec. The amplitude of the sinusoid causes a 34% fluctuation in mass flow rate about the average mass flow rate. The impeller exit area is found to exhibit high fluctuation for both speed ratios. This flow pattern is thought to occur as the high static pressure region above the gap region transitions into the low static pressure region in the impeller passage near the exit.

4. Conclusion

Transient mass flow rate values for two planes under two operating conditions were determined. The following conclusions can be drawn based on the results of this study:

1) The sinusoids have a periodicity that is the same as the period of the turbine blade passing the impeller passage exit with a frequency of 435 Hz for the 0.4 speed ratio and 180 Hz for the 0.8 speed ratio. This indicates a relationship in the flow with the blade passing event.
2) In Plane 2 there is no difference in phasing between the 0.4 and 0.8 speed ratio data sets. The peaks of the sinusoid fall in the same location for each of the respective speed ratio.
3) Plane 1 has sinusoidal fluctuations that have a phase shift with respect to the Plane 2. This may be due to the deceleration of the flow after exiting the impeller passage or it proximity to the turbine blades themselves.
4) This study has led to a better understanding of flow mechanism within the torque converter and provided the guidance needed for the advancement of improved computational fluid dynamic models.

Acknowledgements

We are grateful to Prof. H. Schock and Dr. K. Lee for many helps throughout this work.

References

1. W. Fister and F. W. Adrian, 1983, "Experimental Researches of Flow in Hydrodynamic Torque Converters", Proceeding of the 7th Conference of Fluid Machinery in Budapest, Hungary, Vol. 1, pp. 210~224.
2. R. R. By and J. E. Maloney, 1988, "Technology Needs for the Automotive Torque Converter-Part 1: Internal Flow, Blade Design, and Performance", SAE Paper No. 880482.
3. H. M. Bahr, , R. D. Flack, R. R. By and J. J. Zhang, 1990, "Laser Velocimetry Measurements in the Stator of a Torque Converter", SAE Paper No. 901769.
4. R. R. By and B. Lakshminarayna, 1995, "Measurement and Analysis of Static Pressure Field in a Torque Converter Pump", Journal of Fluids Engineering, Vol. 117, pp. 109~115.
5. J. K. Gruver, R. D. Flake and K. Brun, 1996, "Laser Velocimeter Measurements on the pump of an Automotive Torque Converter: Part I Average Measurements", Trans. of ASME, Vol. 118, pp. 562~569.
6. L. Dalimonte, M. Foster, M. Novak, K. Lee, and H. Schock, 1998, "Measurements of Flows in the Impeller and Turbine Side of an Automotive Torque Converter at 0.4 and 0.8 Speed Ratio", Thesis, Michigan State University, E. Lansing, Michigan.
7. B. Lakshminarayna and T. W. Backstorm, 1996, "Perspective: Fluid Dynamics and Performance of Automotive Torque Converters: An Assessment", Journal of Fluids Engineering, Vol. 118, pp. 665~676.
8. J. K. Gruver, R. D. Flake and K. Brun, 1996, "Laser Velocimeter Measurements on the pump of an Automotive Torque Converter: Part II Unsteady Measurements", Trans. of ASME, Vol. 118, pp. 570~577.
9. S. C. Yoo, 2007, "In-Cylinder Air Flow Measurements and Turbulent Kinetic Energy Analyses", Journal of the Korea Society for Power System Engineering, Vol. 11, No. 4, pp. 5~11.